Diel metabolic patterns in a migratory oceanic copepod

Ann M. Tarrant[1]*, Nora McNamara-Bordewick[1], Leocadio Blanco-Bercial[2], Andrea Miccoli[2,3], Amy E. Maas[2]*

[1] Biology Department, Woods Hole Oceanographic Institution, Woods Hole, MA, USA

[2] Bermuda Institute of Ocean Sciences, St. George's, Bermuda

[3] Department for Innovation in Biological, Agro-Food and Forest Systems, University of Tuscia, Viterbo, Italy

* co-corresponding authors, equal contributions.

Author email and ORCiD

AMT: atarrant@whoi.edu; 0000-0002-1909-7899

NM-B: nkm2123@barnard.edu; no ORCiD (undergraduate researcher)

AEM: amy.maas@bios.edu; 0000-0002-3730-2876

LB-B: Leocadio@bios.edu; 0000-0003-0658-7183

AM: andrea.miccoli@unitus.it; 0000-0002-4545-7229

Running head: Copepod metabolism during diel migration

Keywords: active flux, DVM, excretion, fecal pellets, respiration

Abstract

Diel vertical migration of zooplankton profoundly impacts the transport of nutrients and carbon through the water column. Despite the acknowledged importance of this active flux to ocean biogeochemistry, these contributions remain poorly constrained, in part because daily variations in metabolic rates are not considered or are modeled as simple functions of temperature. To address this uncertainty, we sampled the subtropical copepod *Pleuromamma xiphias* at 4- to 7-hour intervals throughout the daily migration and measured rates of oxygen consumption, ammonium excretion, fecal pellet production and metabolic enzyme activity. No significant patterns were detected in rates of oxygen consumption or ammonium excretion for freshly caught animals over the diel cycle. Fecal pellet production was highest during mid-night, consistent with several hours of feeding near the surface. Surface feeding resulted in fecal pellet production at depth in the morning, providing direct evidence that active flux of particulate organic carbon occurs in this region. Electron transport system activity was highest during the afternoon, contrary to our prediction of reduced daytime metabolism. Activity of both glutamate dehydrogenase and citrate synthase increased during early night, reflecting higher capacity for excretion and aerobic respiration, respectively. Overall, these results show that activities of metabolic enzymes vary during diel vertical migration. The surprising observation of elevated afternoon enzyme activity coupled with daytime fecal pellet and ammonium production suggests that additional characterization of the daytime activity of migratory zooplankton is warranted.

1. Introduction

Diel vertical migration (DVM) of zooplankton is typified by the presence of migrators in the photic epipelagic during the night followed by their movement into deeper water during the day. These daily migrations, during which individuals of a few millimeters in length or less travel hundreds of meters in a few hours, are thought to be energetically expensive. Although costly, this typical pattern of migration is primarily driven by avoidance of predators, particularly visual predators at shallow depths during daytime, and the pursuit of prey (Antezana 2009; Gliwicz 1986; Hays 2003; Pinti et al. 2019).

DVM is a key component of the biological pump (Siegel et al. 2016). Migrators release surface-derived carbon and nutrients as respiratory CO_2 and other excretory waste products (e.g., urea, ammonium, fecal matter, and dissolved organic compounds) below the thermocline (Longhurst et al. 1990; Longhurst and Harrison 1988; Maas et al. 2020; Zhang and Dam 1997). This process, known as active flux, has been estimated to account for 15 - 40% of the total global organic carbon export from the surface to the mesopelagic (Aumont et al. 2018; Bianchi et al. 2013; Steinberg et al. 2000). Through the excretion of nitrogenous compounds at depth, DVM also reduces the availability of this limiting nutrient to phytoplankton in surface waters, influencing the potential for new production (Longhurst and Harrison 1988). In many cases, this daily shuttling of material meets or exceeds the vertical transport associated with passively sinking particles (Hernández-León et al. 2019b; Kobari et al. 2013; Steinberg et al. 2008). At depth, some zooplankton species also consume particles, aggregates, and one another, significantly modifying the availability and export of nutrients and carbon from the mixed layer (Robinson et al. 2010; Schnetzer and Steinberg 2002a). The magnitude and relative importance of active transport varies regionally and seasonally, but the factors driving this variation are poorly

understood (Burd et al. 2010; Steinberg and Landry 2017) and have been identified as a priority for future research on the biological pump (Burd et al. 2016).

Estimates of active flux are typically made by measuring biomass of the migratory community then applying mass-specific and temperature scaling factors (i.e., Q_{10} relationships) to experimentally calculated O_2 consumption rates, as well as organismal nitrogen and carbon excretion rates (e.g., Kiko et al. 2020; Le Borgne and Rodier 1997). However, depth-dependent metabolic rates are driven not only by temperature differences, but also by differences in swimming activity and oxygen availability (Bianchi et al. 2013; Hernández-León et al. 2019a; Herrera et al. 2019). Daily cycles in feeding activity would also be expected to affect metabolic rates through specific dynamic action, the metabolic costs of assimilating nutrients and incorporating them into biomass (Kiørboe et al. 1985). In addition, a few studies in krill and copepods have identified circadian cycles in respiration rate, swimming behavior and the expression of metabolic genes (Häfker et al. 2017; Maas et al. 2018; Teschke et al. 2011). If these patterns are widespread and there are cycles in other major physiological processes, like fecal pellet production and ammonium excretion, they may cause substantial errors in the estimations of organismal contributions to biogeochemical flux during daytime at depth.

In addition to direct metabolic measurements of oxygen consumption, nitrogen excretion and fecal pellet production, aspects of active flux have been estimated by measuring the activity of key enzymes including the electron transport system (ETS) for respiration or glutamate dehydrogenase (GDH) for ammonium excretion (Bidigare 1983; Fernández-Urruzola et al. 2011; Hernández-León et al. 2019a; Packard and Gómez 2013). Such measurements have the advantage that they avoid artifacts associated with bottle incubations, but it is unclear over what time scale the fluctuations in enzymatic activity correspond to changes in organismal metabolic

rates. Predictions of organismal metabolic rates from enzymatic activity measurements of field-collected zooplankton typically have large uncertainties, e.g., 31-38% for O_2 consumption and ETS (Packard and Gómez 2013; Packard et al. 1988) and 42.5% for ammonium excretion GDH (Fernández-Urruzola et al. 2016). Part of this uncertainty can be explained by variation in physiological activity and metabolic rates as a percentage of the maximum rate that could be supported by a given enzyme. For example, food availability and quality affect substrate availability, and contribute to decoupling between measurements of oxygen consumption and ETS activity (Hernández-León and Gómez 1996; Osma et al. 2016).

For organisms that undergo DVM, daily cycles in food availability are somewhat predictable, so they might modulate their enzymatic capacity in anticipation of this variability. Daily physiological and behavioral cycles can be directly triggered by environmental conditions, and can also be regulated through endogenous circadian clocks. In nature, these two mechanisms are interrelated because circadian clocks are entrained by environmental cues, such as light, temperature and food availability. Conserved components of the circadian clock have been identified in a few planktonic crustaceans, including the euphausiids *Euphausia superba* (Teschke et al. 2011, De Pitta et al. 2013) and *Meganyctiphanes norvegica* (Blanco-Bercial and Maas 2018), and the copepods *Calanus finmarchicus* (Christie et al. 2013, Häfker et al. 2017) and *Pleuromamma xiphias* (Maas et al. 2018). In *E. superba* and *C. finmarchicus,* circadian cycles in expression of circadian regulatory genes, metabolic enzymes (e.g., citrate synthase), and oxygen (O_2) consumption have been described, and similar daily cycles have been detected in field populations (Teschke et al. 2011, De Pitta et al. 2013, Häfker et al. 2017). While external environmental cues have a large direct influence on DVM, laboratory experiments with krill (Gaten et al. 2008), copepods (Hüppe 2016) and nereid worm larvae (Tosches et al. 2014)

suggest that circadian pathways can also contribute to this behavior. Regardless of the relative importance of circadian regulation versus direct responses to the environment, knowing when particular metabolic pathways are activated would allow prediction of when and where their end products are released into the water column, contributing to active flux transport and providing important nutrients to the midwater.

To address these knowledge gaps, we investigated daily physiological changes in the copepod *Pleuromamma xiphias* (Giesbrecht, 1889), which is abundant, occurs throughout the tropical and subtropical oceans, and exhibits a strong diel vertical migration (Goetze 2011 and references therein). The contributions of *P. xiphias* to nitrogen and carbon flux have previously been characterized using classical bottle sampling methods and abundance estimates (i.e. Steinberg et al. 2000; Steinberg et al. 2002; Teuber et al. 2013). At the Bermuda Atlantic Time-series (BATS) site, near the sampling site of our study, seasonal measurements have indicated that *P. xiphias* is the most biogeochemically relevant of the *Pleuromamma* copepods in the region. Together these copepods and the euphausiid *Thysanopoda aequalis* make up 23% of the surface zooplankton biomass on average, suggesting that they are the most important contributors to active flux (range 4-70%; Figure 3 within Steinberg et al. 2000). We have previously shown that *P. xiphias* exhibits a circadian pattern in oxygen consumption when held under constant laboratory conditions, with a peak during dawn and lowest levels during the evening (Maas et al. 2018). In the present study, diel metabolic variation of *P. xiphias* was examined in the natural context of its daily migration using organismal metabolic measurements, as well as enzymatic activity assays. We hypothesized that the combined influences of the circadian machinery and the environment would create emergent molecular and physiological cycles that cannot be accounted for solely by Q_{10} relationships. Specifically, we expected that excretion rates would be elevated

during the night and that oxygen consumption rates would be highest at dawn, as we had previously observed. Finally, we predicted that patterns in glutamate hydrogenase activity would mirror ammonium excretion rates and that patterns in citrate synthase and the electron transport system activity would reflect oxygen consumption rates.

2. Materials and Methods

2.1 Sample Collection

Pleuromamma xiphias were collected offshore from the Bermuda Institute of Ocean Sciences (BIOS) during a cruise aboard the *R/V Atlantic Explorer* from May 20-22, 2019 (Figure 1). All times were reported as solar times. On May 21, sunrise occurred at 5:02 and sunset at 18:59; solar noon corresponded to 13:15 Bermuda local time (UTC -3 during Daylight Saving Time). Net tows were conducted at 12 time points, spaced 4-7 hours apart to target afternoon, early night, mid-night and morning (Table 1). The timing of morning and early night tows was selected to target recently arrived migrants based on empirical observations from previous tows and the first day of sampling. Nighttime tows (early- and mid-night) were conducted using a 1-m^2 Reeve net (Reeve 1981) deployed to 200 m depth, with 150 µm mesh, a 20-L cod end, and a miniSTAR-ODDI pressure and depth sensor. Daytime tows (morning and afternoon) were conducted using a 1-m^2 MOCNESS with 150 µm mesh and a custom-built thermally-insulated closing cod end. The thermally-insulated cod end was used because copepods were also sampled for transcriptomic and proteomic analyses that will be presented elsewhere. Because the goal of the MOCNESS sampling was to collect copepods from a single depth stratum, only one closing net was used each time to sample from 400-600 m depth. To obtain temperature profiles, CTD rosette casts were conducted prior to six of the net tows using a Seabird 911 CTD equipped with

additional oxygen, fluorescence, turbidity and backscatter sensors. After each tow, copepods were examined under a Leica M205 C stereomicroscope to identify adult *P. xiphias* and determine their sex. Copepods were either used immediately for respirometry and excretion measurements or flash-frozen for subsequent enzyme activity measurements.

2.2 Organismal Metabolic Measurements

Water for physiological experiments was obtained daily from 120 m depth using the rosette on the CTD. It was gravity filtered past a 0.2 µm Supor filter in a Georig 142 mm filter holder and equilibrated to 20°C in an upright incubator. Two types of experiments were conducted. In the first, rates of oxygen consumption, ammonium excretion and fecal pellet production were measured at four time points per day (discrete incubations). In the second, ammonium, urea and DOC excretion were measured from individual copepods over time (time-course measurements).

2.2.1 Discrete incubations over a daily cycle

At each time point (four per day), up to six copepods were transferred into individual respiration chambers (i.e., one animal per chamber) that consisted of 50-mL glass syringes containing an optically sensitive oxygen sensor (OXFOIL: PyroScience, Aachen Germany) and 30 mL of 0.2 µm filtered seawater. A glass bead was placed at the bottom of each syringe to avoid trapping the copepod in the small region of the syringe outlet, and all air bubbles were purged from the chamber. To control for bacterial respiration, two chambers were filled with water but were left without a copepod. Chambers were placed upright (plunger facing upward) in a dark 20°C incubator, and the oxygen concentration in each chamber was measured non-invasively and continuously (every 60 seconds) for approximately 3 hours using two FireSting optical oxygen meters (PyroScience, Aachen Germany), initialized with a 2-point calibration procedure (100%

air-saturated water and 0% oxygen-free water by sodium sulfite reaction) on May 19, 2020. At the end of the experiment, the chambers were visually inspected to ensure that the copepods were still swimming. A 15-mL subsample of water was filtered at a 30º upward angle (to avoid damaging copepods or fecal pellets) through 0.7 µm GFF filters into 15-mL conical vials that had been pre-treated with o-phthalaldehyde (OPA) working reagent (21 mM sodium tetraborate, 0.063 mM sodium sulfite, 50 mL L^{-1} o-phthalaldehyde in ethanol). This filtered water was refrigerated (4°C) for less than 24 h and then ammonium concentration was assayed at sea, as described below. The copepod and any fecal pellets from each chamber were rinsed into a petri dish. Fecal pellets were counted and photographed under a stereomicroscope. Copepods were rinsed once in deionized water and frozen at -80ºC. Frozen copepods were subsequently weighed on a Mettler-Toledo XPR microbalance, dried, and reweighed.

Individual respiration rates were corrected for bacterial respiration by plotting the oxygen concentration (µmol O_2 L^{-1}) in each chamber over time then subtracting the mean slope (reduction in oxygen per hour) of the controls from those of each organismal chamber to provide the respiration rates. Rates were corrected for chamber volume and copepod dry mass (µmol O_2 mg_{DM}^{-1} h^{-1}).

Ammonium was measured using the OPA method (Holmes et al. 1999). Each day, a standard curve (0-3 µmol L^{-1}) was created in duplicate, and refrigerated samples were equilibrated to room temperature. Samples and standards were then spiked with the working reagent and were maintained in the dark for 3 h prior to analysis on a Turner fluorometer with the ammonium module (1 cm path length cuvette). Ammonium concentration was calculated based on the linear equation generated by the standards and corrected for background fluorescence. This value was

adjusted by chamber volume, experimental duration, and copepod dry mass (μmol NH_4^+ mg_{DM}^{-1} h^{-1}).

Oxygen consumption rate, ammonium excretion rate, and dry mass were measured for 60 copepods (n= 10-18 per time point, 40 females, 19 males, and 1 juvenile CV female). Log-transformed rates of oxygen consumption and ammonium excretion were compared across timepoints (i.e., 4 times, pooled across days) using ANCOVA with log-transformed mass as a covariate (SPSS version 22). Equality of variances was confirmed with Levene's test. Differences in fecal pellet production between timepoints was assessed using the nonparametric independent-samples median test. Significance of all analyses was assessed at $p < 0.05$.

2.2.2 Time-course excretion measurements

Two experiments were conducted to measure ammonium excretion by *P. xiphias* over time. For the first, copepods were collected from repeated Reeve tows from 19:45 to 22:45, and for the second copepods were collected from a single Reeve tow at 19:45. Copepods were placed into individual pre-filled ~115-mL pre-combusted glass jars at 23:15 for both experiments, which were incubated in the dark at 20°C. Every six hours, five experimental jars and one control jar (with the same water but no copepod) were sampled using a positive pressure system past a 0.2 micron polytetrafluoroethylene (PTFE) filter. The 10-mL samples were stored in 15-mL conical vials that were pre-treated with OPA working reagent, and ammonium concentration was measured daily in the samples, as described in section 2.2.1. Changes in ammonium concentrations and excretion rates were analyzed via linear regression.

2.3 Enzyme Assays

For enzyme activity measurements, copepods were thawed on ice, blotted on a tissue, and quickly weighed on a Cahn C-33 microbalance. Groups of 2-5 copepods were pooled into 300 µL of ice-cold enzyme-specific buffer in a 5-mL Potter-Elvehjem homogenizer. Copepod tissue was homogenized using a motorized PTFE pestle for two 30-second bursts with 30 seconds of ice cooling between bursts. Homogenates were centrifuged at 14,000g for 20 minutes at 4°C, and the supernatant was retained. Protein concentration was measured in the supernatant using the Bradford protocol (Bradford 1976). Except where noted, enzyme activity measurements were made with 20 µL homogenate per well in triplicate wells of a 96-well plate. Measurements were made at 26°C using a SpectraMax plate reader. The automix function was used prior to each set of measurements.

The assay for glutamate dehydrogenase (GDH) is based on the rate of oxidation of NADH (Willett and Burton 2003). Copepods were homogenized in buffer (100 mM Tris pH 8, 50 mM NH_4Cl, 10 mM EDTA, 0.0025% Tween-80), as described above. Then 180 µL of GDH assay buffer (200 µM ADP, 100 µM NADH in GDH homogenization buffer, made fresh daily) was added to the homogenate. Baseline absorbance was monitored for 8 minutes at 340 nm to ensure depletion of endogenous substrates. To measure enzymatic activity, 20 µL of substrate (5 mM α-ketoglutarate) was added to each well, and the change in absorbance at 340 nm was recorded over 8 minutes.

Citrate synthase (CS) activity was measured modifying the protocol of Hawkins et al. (2016). Copepods were homogenized in buffer (25 mM Tris, pH 7.8, 1mM EDTA, 10% glycerol). 170 µL of CS assay buffer (0.11% Triton X-100, 294 µM 5,5'-dithiobis-[2-nitrobenzoic acid] [DTNB], 588 µM acetyl-coenzyme A in CS homogenization buffer, made fresh daily) was added to the homogenate. After taking baseline absorbance measurements for 3 minutes at 405 nm, 10

242 µL of 10 mM oxaloacetate was added to each well, and the change in absorbance at 405 nm was
243 recorded over 3 minutes.

244 Electron transport system (ETS) activity was measured modifying the protocol of Owens and
245 King (1975). Aliquots of the same homogenates from the CS assay were diluted 1:3 in ETS
246 phosphate buffer (0.1 M, pH 8.5, Na_2HPO_4, KH_2PO_4, Triton X-100). 40 µL of each diluted
247 sample was added in triplicate along with a fourth aliquot used as a no-substrate control,
248 followed by 120 µL of ETS assay buffer (1.25 mM NADH and 0.22 mM NADPH in phosphate
249 buffer, made fresh daily) to the samples or 120 µL of phosphate buffer alone to the control wells.
250 After taking baseline absorbance measurements for 8 minutes at 490 nm, 40 µL of 0.2% 3-(4-
251 iodophenyl)-2-(4-nitrophenyl)-5-phenyl-2H-tetrazol-3-ium chloride (INT), pH 8.5 was added to
252 each well, and the change in absorbance at 490 nm was recorded over 8 minutes.

253 Citrate synthase activity was determined by comparing measurements of copepod homogenates
254 with a standard curve derived from a dilution series of a pure enzyme standard (citrate synthase
255 from porcine heart, Sigma-Aldrich). Other enzymatic activities were calculated using the Beer-
256 Lambert Law with extinction coefficients of 6.22 mM^{-1} cm^{-1} for NADH (GDH, reported by
257 Sigma-Aldrich, the supplier) and 15.9 mM^{-1} cm^{-1} for INT (ETS assay, as in Owens and King
258 1975). The enzyme activity measurements were not conducted on the same copepods used in
259 individual measurements of oxygen consumption and ammonium excretion, so the values do not
260 represent calibrated activity rates.

261 Enzyme activity measurements were separately normalized to dry mass and to protein. Dry mass
262 was calculated as 0.0513 times wet mass, based on the average ratio from measurements in the
263 respirometry experiences (n = 61). Physiological and enzymatic measurements were log10-

transformed prior to analysis. Differences in enzymatic activity of pooled copepod samples were analyzed using a one-way ANOVA (using the oneway.test function in R, which does not assume equal variances) with a Games-Howell post-hoc test to identify significantly different groups ($p < 0.05$).

3. Results

3.1 Site characteristics and sample description

Throughout the sampling period, a deep chlorophyll maximum (DCM) consistently occurred around 130-160 m depth; thus, nighttime sampling (to 200 m depth) would have included copepods feeding within this region (Figure 2). Temperature was 23-24°C at the surface, 20°C at the DCM, and 17-18°C at 500 m depth. Oxygen levels decreased with depth, but were always above 160 μmol kg^{-1} at the depths sampled. The exact timing of the tows and incubations varied from day to day (Table 1). Timepoints were clustered into four groups sampled at the same depth range and similar times of tow recovery (R) and incubation start (I): morning (R: 6:25-7:38; I: 7:35-8:30), afternoon (R: 12:52-13:27; I: 13:50-14:55), early night (R 17:31-19:04; I: 21:25-21:45), mid-night (21:00-22:55; I: 1:15-2:45). The delay between each tow recovery and the start of the corresponding incubation primarily represented the time required to identify sufficient adult females for all study objectives.

3.2 Organismal Metabolic Measurements

There was no significant difference among time points in the mass-normalized rates of oxygen consumption or ammonium excretion (Fig. 3A-B, oxygen consumption $F(55,3) = 0.242$, $p = 0.867$; ammonium excretion $F(55,3) = 0.545$, $p = 0.653$). Rates did not vary by sex, and the

interpretation was not changed by limiting the analysis to adult females (not shown). Fecal pellet production varied significantly over the course of the day with maximum values at mid-night that were significantly higher than afternoon or early night (Fig. 3C, $X^2(3, N = 64) = 20.426$, $p < 0.001$). The fecal pellets produced at mid-night appeared densely packed and were brown or green in color. Some of the fecal pellets produced during daytime were similar in appearance; however, others were light-colored and loosely packed (Fig. 4).

In the time-course studies, ammonium concentrations increased over time, indicating some continued excretion over the 18-hour incubation (Fig. 5A). There was not a statistically significant change in the integrated rate of excretion measured at each sampling point (Fig. 5B), but mean ammonium excretion rates decreased with each sampling interval (Fig 5C).

3.3 Enzyme Activity Measurements

Patterns of enzyme activity were broadly similar whether the data were normalized to wet mass (Fig. 6) or protein concentration (Supplemental Figure 1); however, the statistical significance varied with the method of normalization (Table 2). ETS and CS both exhibited significant differences in activity over time when normalized to mass, though the patterns were different (Figs. 6A and 6B, respectively). Within the deep water, ETS activity was higher during the afternoon than during the morning; this was contrary to our hypothesis that rates would be highest during morning. CS was highest at night, with significant differences between early night and both the daytime points. GDH activity also tended to be higher at night, with a significant increase between afternoon and early night when normalized to protein (Table 2, Supplemental Fig. 1). Mean activity at night was approximately twice the afternoon activity at depth, and this difference would be magnified in the field due to differences in temperature with depth.

4. Discussion

Over a three-day period, *Pleuromamma xiphias* copepods were sampled from depths that corresponded to their typical diel vertical migration. Fecal pellet production and ammonium excretion during daytime at depth were consistent with both active transport and some degree of midwater feeding. Daily patterns in enzymatic activity suggest that the copepods respond to or anticipate differences in food availability, temperature and/or other environmental conditions over the course of the migratory cycle.

We did not observe significant variation in oxygen consumption rate during our discrete measurements of respiration. Our failure to detect a diel rhythm in oxygen consumption in wild-caught animals was initially surprising, given previous reports of circadian rhythms in copepod respiration (Häfker et al. 2017; Maas et al. 2018); however, the present study was very different in design and goals than the previous circadian studies. The previous circadian studies consisted of continuous longitudinal measurements of oxygen utilization, whereas the present eco-physiological study consisted of independent samples collected directly from the field. Thus, rates measured in the current study reflect the combined influences of circadian patterns in physiology, as well as the variable feeding and swimming history of the individuals over their vertical migration.

Unexpectedly high inter-individual variability among samples in the current study may have prevented detection of a diel cycle in oxygen consumption rate. To provide context, the amplitude of the circadian cycle we previously reported in *P. xiphias* oxygen consumption rates (initially 173 μmol g^{-1}_{DM} h^{-1} with rapid dampening; Maas et al. 2018) is similar in magnitude to the difference (non-significant) in means between morning and afternoon observed in the present

study (128 μmol g^{-1}_{DM} h^{-1}). To detect a difference of this magnitude (128-173 μmol g^{-1}_{DM} h^{-1}) given the observed variability of the field-collected samples (mean standard deviation of time points 140 μmol g^{-1}_{DM} h^{-1}) we approximate a required sample size of 21-29 (α= 0.05, β=0.80; based on ANOVA of mass-normalized samples with 6 pairwise comparisons, Chow et al. 2007), a substantial increase from our actual sample size of 10-18 per time point. Our results also contrast previous observations by Pavlova (1994), who conducted endpoint measurements that were similar to those used in the present study, and who observed greatly increased respiration rates by *P. xiphias* around dawn and dusk. However, the oxygen consumption rates measured at dawn and dusk by Pavlova (1994) are an order of magnitude greater than any respiration rates observed for *P. xiphias* adults in several subsequent studies (Maas et al. 2018; Steinberg et al. 2000; Teuber et al. 2013). While we cannot provide a definitive explanation for this discrepancy, possible explanations could be unique physiology of the populations sampled by Pavlova (e.g., sampling was done from individuals captured at 5 m depth in the Indian Ocean, where there is a strong oxygen minimum zone), a failure of this study to make measurements during ephemeral periods of peak respiration, or methodological artifacts (e.g., differences in handling stress).

Fecal pellet production rates were highest during mid-night, but there was also some evidence of daytime feeding with occasional pellets even in the afternoon. Our results suggest a 50% decrease in production rate of fecal pellets when comparing mid-night (0-200 m depth) and early morning (400-600 m depth). This is consistent with the estimates made by Schnetzer and Steinberg (2002b) who estimated 57% production of surface-derived fecal pellets by *P. xiphias* at 300 m depth using gut evacuation rate experiments and migration speed**.** *Pleuromamma xiphias* has been demonstrated to commonly have > 50% of their gut contents consisting of material suspected to be of detrital origin (Schnetzer and Steinberg 2002a), which might imply

that substantial feeding activity could occur continuously throughout the water column and over the full diel cycle. However, the observed reduction in fecal pellet production at depth during the day suggests that midwater feeding is substantially less than surface nighttime consumption. Although validation of the origin of these pellets would require isotopic, microscopic or molecular analysis of their content, the similarity in the morphology of many of the mid-night (surface) and early morning (deep) fecal pellets suggests instead that at least some of these pellets are derived from surface feeding. These would then contribute to particulate organic carbon active flux, as predicted by Schnetzer and Steinberg (2002b).

Ammonium excretion rates dropped over an eighteen-hour incubation (time-course measurements) but exhibited no variation over the course of the day (discrete incubations). The decreasing rate in the time-course measurements likely reflects reduced excretion as food in the gut is cleared, suggesting that feeding only at the surface during night would not be sufficient to sustain continued excretion over the full daily cycle. Thus, when taken in conjunction with the time series results, the lack in diel variation is intriguing and would be consistent with continued feeding at depth to support continued ammonium excretion in the field-caught samples.

While we did not detect diel changes in organismal-level measurements of oxygen consumption and ammonium excretion rates, there were diel changes in the activity levels of the three metabolic enzymes measured. This discrepancy could reflect the interplay between enzyme activity measurements and substrate availability that resulted in consistent metabolism despite variations in enzymatic capacity. Alternatively, the enzymatic measurements, which were made on rapidly flash-frozen individuals, may have been less impacted by the effects of handling or captivity that were associated with the experimental incubations needed to measure organismal rates.

ETS activity is generally considered to reflect the value of oxygen consumption if all enzymes in the electron transport chain were functioning at maximum activity, whereas *in vivo* respiration rate may be constrained by substrate limitation or the presence of inhibitors. While oxygen consumption rates and ETS activity are often concordant (e.g., Bidigare 1983; Maldonado et al. 2012; Packard 1985), they can respond differently to changes in food availability, temperature and other factors (Hernández-León and Gómez 1996; Osma et al. 2016). Unlike respiration rate, which was consistent throughout the diel cycle, ETS activity in our study was significantly higher in the afternoon than in the morning. The increase in ETS activity between morning and afternoon is puzzling, as our previous work with this species demonstrated a circadian peak in oxygen consumption rates in the morning (6-12 h) and the lowest respiration rate in the early evening (18-24 h) under constant conditions in the laboratory. Multiple additional environmental factors could be influencing the *in situ* ETS expression, but the patterns cannot be clearly explained by predicted changes in swimming activity or metabolic changes due to specific dynamic action associated with food processing. Experimental studies with the copepod *Acartia tonsa* demonstrated that copepods maintained high rates of metabolism for about 8 hours after removal for food (Kiørboe et al. 1985). While this timing may be expected to vary among copepod species, a metabolic pattern driven solely by feeding activity and postprandial metabolic processes would be expected to have the lowest rates during the afternoon sampling period. Alternatively, the higher ETS capacity may be a strategy used to offset the Q_{10} temperature effect, allowing for sustained aerobic metabolism despite lower midwater temperatures. While such a compensatory effect is consistent with elevated ETS activity observed during afternoon, it does not explain the low expression in the morning period. A third possibility is that the copepods are upregulating their metabolic capacity in preparation for their nighttime ascent.

Analogous anticipatory rhythms have been characterized in model organisms, such as mammalian food anticipatory behavior (increased actiivity 1-3 hours before meal time; reviewed by Silver et al. 2011) and anticipatory upregulation of catabolic liver enzymes (Díaz-Muñoz et al. 2000).

When comparing studies of diel metabolism of migratory zooplankton, there is a consistent disconnect between observed patterns in respiratory peaks, which are often coincident with sunrise and sunset (Häfker et al. 2017; Maas et al. 2018; Pavlova 1994), and the period of highest ETS expression. Although the precise peak in ETS activity differs among the migrating species that have been examined, it is consistently during the daytime portion of the diel cycle. For example, a study of euphausiid physiology in an area with a pronounced oxygen minimum zone found peak ETS activity levels during early morning in animals caught at depth (400-500 m depth; Hernández-León et al. 2019b). A pattern more similar to that detected in our study was observed in a laboratory-based study of krill by Biscontin et al. (2019), who report peak late-afternoon expression of genes associated with the electron transport chain and Krebs cycle. The discordance between ETS and respiration measurements and the variation in peak timing observed in studies conducted in different species and ecosystems together suggest a need for greater coordinated study, particularly since ETS measurements are used as a proxy for respiration in biogeochemical studies (Belcher et al. 2020; Hernández-León et al. 2019b; Hernández-León et al. 2019c; Packard and Gómez 2013).

Alternate enzymatic proxies for respiration include individual enzymes within the citric acid cycle, the reactions which provide high-energy electrons to the ETS. Of these, citrate synthase (CS) is the first enzyme of the citric acid cycle that performs the irreversible condensation of acetyl-CoA with OA to create citrate. Unlike the ETS machinery, the activity of CS in our study

421 was elevated during nighttime, when *P. xiphias* is expected to be feeding most actively. High
422 rates of nighttime feeding are consistent with observed increases in fecal pellet production during
423 the mid-night period. Citrate synthase has been used to indicate aerobic metabolic potential but
424 does not always correlate well with oxygen consumption rates in invertebrates (Thuesen et al.
425 1998 and references therein). In copepods, previous studies have correlated CS activity with
426 food availability on multiday timescales (e.g., 2-3 day lab incubations, Clarke and Walsh 1993;
427 pre-/post-bloom Geiger et al. 2001). Daily patterns in CS (i.e., cycles *within* days) have not been
428 previously described in copepods, but are well-documented in mammalian tissues through
429 measurements of both transcript expression and enzymatic activity (Crumbley et al. 2012; Glatz
430 et al. 1984). Among other zooplankton, both circadian and ultradian patterns of CS expression
431 have been observed in krill (Biscontin et al. 2019; De Pittà et al. 2013; Teschke et al. 2011).
432 Meyer and colleagues (2010) suggested that malate dehydrogenase (MDH), another enzyme in
433 the citric acid cycle that additionally shunts electrons between cytosolic and mitochondrial
434 compartments, might better correspond to oxygen consumption rates. Diel patterns in copepod
435 MDH expression have not yet been investigated and would be useful to include in future studies;
436 however, seasonal studies in both copepods and euphausiids have indicated a general
437 correspondence of both CS and MDH activity with oxygen consumption rates (Freese et al.
438 2017; Meyer et al. 2010).

439 Glutamate dehydrogenase (GDH), which mediates the production of ammonium waste during
440 amino acid catabolism and is associated with the urea cycle, exhibited peak activity at night. This
441 contrasts with direct measurements of ammonium excretion, which showed no pattern. A
442 possible explanation for the discrepancy between ammonium and GDH measurements could be
443 artifacts in the ammonium measurements due to stress of capture, handling, captivity (small

chamber size) and acclimation to starved conditions (Ikeda et al. 2000; Kodama et al. 2015). In addition, while GDH activity is used as a proxy for potential excretion rate, actual excretion rate may be limited by substrate availability (Fernández-Urruzola et al. 2016). We are not aware of any other studies tracking GDH activity during diel vertical migration. Bidigare et al. (1983) measured depth-stratified GDH activity of bulk zooplankton communities within the upper 200 m depth in the Gulf of Mexico. The highest activities occurred within the mixed layer and were largely driven by zooplankton abundance. Protein-specific activity was only reported during the daytime and was highest in the upper 100 m. Within the first 24-hours of laboratory incubations with starved mysids, Fernandez-Urruzola et al. (2011) found an initial increase in ammonium excretion, followed by a sharp decrease; however, they observed high variability in GDH activity within time points and no consistent temporal patterns. The design of the mysid study was quite different from the present study in that a single cohort of animals was brought into the laboratory and sampled over time. Despite these differences, it supports the idea that zooplankton excretion rates could change on a daily scale with feeding activity.

To date, the handful of previous studies that have characterized aspects of circadian metabolism in zooplankton have been conducted using a limited range of taxa, primarily copepods (Häfker et al. 2017; Maas et al. 2018; Pavlova 1994) and krill (Biscontin et al. 2019; De Pittà et al. 2013; Teschke et al. 2011). Further, most of this work has been conducted in polar or sub-polar environments. Consequently, assessing diel rhythms in multiple species across a range of environments will be important as we seek to better understand the cycling of nutrients in the euphotic and twilight zone. The studies cited above used a combination of methods including organismal physiology (e.g., oxygen consumption, ammonium excretion), transcriptomics, proteomics, and enzyme activity assays. Each of these approaches can provide insight into the

467 physiological ecology of zooplankton and zooplankton contributions to biogeochemical cycling;
468 however, these types of measurements are subject to different sources of error and may indicate
469 variability over different time scales. Moving forward, disentangling which factors these
470 measurements are responding to (e.g., light, temperature, oxygen concentration, food
471 availability, endogenous circadian rhythms,) will help us to better apply these tools to quantify
472 zooplankton contributions to biogeochemical cycles.

473 **5. Conclusions**

474 This study demonstrates that the copepod *Pleuromamma xiphias* exhibits variation in fecal pellet
475 production and activity of metabolic enzymes as it undergoes diel vertical migration, supporting
476 our hypothesis that circadian rhythms and other environmental factors beyond temperature create
477 emergent patterns in zooplankton physiology. Observed production of fecal pellets in deep water
478 during morning indicates that surface feeding by migratory copepods contributes to active flux of
479 particulate organic matter. Occasional late afternoon fecal pellets and sustained levels of
480 ammonium excretion by copepods sampled during daytime suggests continued, although
481 reduced, levels of midwater feeding. Despite the diel patterns in enzyme activity, there were no
482 statistically significant variations in oxygen consumption or ammonium excretion over the diel
483 cycle. Studying diel rhythmicity in physiological rates (respiration, ammonium excretion)
484 remains difficult in field-caught organisms, yet further studies are needed both in *P. xiphias* and
485 in other migratory species. Enzyme activity assays can complement direct physiological
486 measurements, and the observed daily variation in metabolic enzymes indicates that copepods
487 adjust their metabolic capacity in response to or perhaps in anticipation of variation in
488 environmental conditions and metabolic demands. However, measurements of enzymatic activity
489 indicate peaks in metabolic potential that may lead or lag actual cycles in physiological rates;

this decoupling can contribute to uncertainty in applying enzymatic measurements to estimate zooplankton contributions to respiration and ammonium production.

Data Archiving

CTD profiles and physiological data are available through the Biological and Chemical Oceanography Data Management Office (BCO-DMO); https://www.bco-dmo.org/project/764114.

Acknowledgements

We thank Captain George Gunther and the crew of the R/V *Atlantic Explorer*. We thank Hannah Gossner, Emma Timmins-Schiffman, Lindsey Cunningham, Susanne Neuer, Brook Nunn, and Brittany Widner for assistance with sampling. We are grateful for the advice and assistance of Peter Wiebe during the design and testing phase of the closing cod end. We also thank the anonymous reviewers for their constructive comments on this manuscript.

Funding

This work was supported by the National Science Foundation [Grant OCE-1829318 to AEM, AMT and LBB]. Support for NM-B was provided by the Woods Hole Oceanographic Institution's Summer Student Fellows Program. These funders played no role in decisions related to the study design, implementation or interpretation.

CRediT author Statement

Ann M. Tarrant: Conceptualization, Funding Acquisition, Investigation, Supervision, Writing - Original Draft, Writing - Review & Editing. **Nora McNamara-Bordewick**: Investigation,

Writing - Review & Editing **Leocadio Blanco-Bercial**: Conceptualization, Funding Acquisition, Investigation, Visualization, Writing - Review & Editing **Andrea Miccoli** Investigation, Writing - Review & Editing **Amy E. Maas** Conceptualization, Project Administration, Funding Acquisition, Investigation, Data Curation, Supervision, Writing - Review & Editing.

Figure Legends

Figure 1: (Left) Map showing bathymetry of the sampling region. Black circles mark tow locations. (Right) Regional map showing the position of Bermuda within the North Atlantic Ocean.

Figure 2: Plots of hydrographic conditions on 20 May 2021 at 32º 10.435N, 64° 30.018W (i.e., prior to Tow 1, Table 1). Additional hydrographic data are available at https://www.bco-dmo.org/project/764114.

Figure 3: *Pleuromamma xiphias* physiological rates. Distinct letters indicate statistically distinct time points. Open boxes denote samples collected from depth (400-600 m) during daytime, and solid boxes indicate samples collected from surface waters (<200 m) during night. Oxygen and ammonium rates per gram dry mass (DM) per hour. (A) Oxygen consumption, N=10-19; (B) Ammonium excretion, N=10-18; (C) Fecal pellet production (per 3-hour incubation period), N=13-19.

Figure 4: Examples of fecal pellets produced by *Pleuromamma xiphias* during 3-hour incubations over a three-day period, with sequential sampling points beginning in the upper left and proceeding to the right and down over time.

Figure 5: Time series of *Pleuromamma xiphias* ammonium production from individual copepods that had been captured between 19:45 and 22:45 on May 20th (solid symbols) or between 19:45 and 20:45 on May 22nd (open symbols). Both excretion experiments were set up at ~23:15 and results are reported as time since the start of the experiment (x-axis) with (A) total production; (B) production integrated over time on the y-axis; (C) production per 6-hour sampling window calculated by excluding the average production of the prior time points to

538 demonstrate the excretion rate over the duration of the experiment in relation to solar time. White
539 bars show the average production per time point.

540 Figure 6: Log-transformed enzymatic activity of electron transport system (ETS; A), citrate
541 synthase (CS, C) and glutamate dehydrogenase (GDH, C). Activity normalized to dry mass.
542 Time of sampling and sample size indicated on the x-axis. Open boxes indicate samples
543 collected from depth (400-600 m) during daytime, and shaded boxes indicate samples collected
544 from surface waters (<200 m) during night. Letters indicate statistically distinct time points.

545

546

547 Table 1: Tow sampling data. All times are reported relative to solar noon (12:00).

Timepoint[a]	Type[b]	Date	Nominal Time	Tow Start	Tow Stop	Incubation Start[c]	Lat (N)	Long (W)
1; CTD	Reeve	05/20/19	Early night	16:38	17:31	21:25	32º 10.435'	64° 30.018'
2	Reeve	05/20/19	Mid-night	19:50	21:00	1:15*	32º 08.434'	64° 28.581'
3; CTD	MOC	05/21/19	Morning	5:10	6:25	7:35	32º 10.689'	64° 30.293'
4	MOC	05/21/19	Afternoon	11:50	13:06	14:30	32º 24.363'	64° 28.749'
5	Reeve (2 tows)	05/21/19	Early night	16:44 18:07	17:44 19:04	21:45	32º 33.650' 32º 33.707'	64° 34.754' 64° 34.759'
6	Reeve	05/22/19	Mid-night	21:02	22:00	1:55*	32º 33.387'	64° 33.609'
7	MOC	05/22/19	Morning	6:19	7:38	8:30	32° 31.592'	64° 30.307'
8; CTD	MOC	05/22/19	Afternoon	12:09	13:27	14:55	32º 30.127'	64° 33.194'
9; CTD	Reeve	05/22/19	Early Night	16:43	17:45	21:35	32º 34.141'	64° 38.701'
10	Reeve	05/23/19	Mid-night	21:53	22:55	2:45*	32º 10.416'	64° 47.369'
11; CTD	MOC	05/23/19	Morning	5:57	7:15	8:30	32º 08.950'	64° 47.354'
12; CTD	MOC	05/23/19	Afternoon	11:50	12:52	13:50	32º 13.948'	64° 40.649'

548

549 [a] "CTD" indicates that a tow was directly preceded by CTD profiling.

550 [b] Reeve net tows had a maximum depth of 159 ± 12 m (mean ± SD). MOCNESS (MOC) tows

551 sampled from 400-600 m depth.

552 [c] Asterisk (*) indicates that time corresponds to the day following the start of tow.

553

554 Table 2: One-way Welch's ANOVA and significant post-hoc (Games-Howell) results from
555 enzyme activity assays

Assay	Dry mass-normalized activity	Protein-normalized activity
ETS	$F(3, 7.94) = 4.83$; $p = 0.03$ Morning vs. Afternoon $p = 0.02$	$F(3, 6.88) = 2.75$; $p = 0.12$
CS	$F(3,8.59) = 12.09$; $p < 0.01$ Morning vs. Early Night $p = 0.01$ Afternoon vs. Early Night $p = 0.04$	$F(3,7.80) = 3.36$; $p = 0.08$
GDH	$F(3,8.35) = 3.10$; $p = 0.09$	$F(3, 4.35) = 9.19$; $p = 0.02$ Afternoon vs. Early Night $p < 0.01$

556

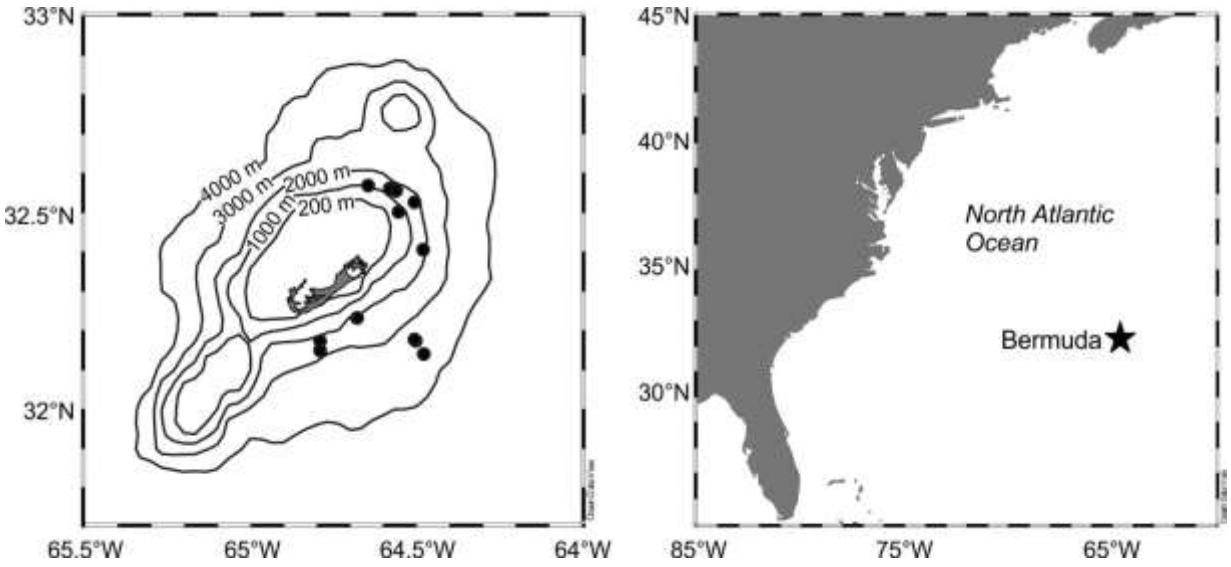

Figure 1: (Left) Map showing bathymetry of the sampling region. Black circles mark tow locations. (Right) Regional map showing the position of Bermuda within the North Atlantic Ocean.

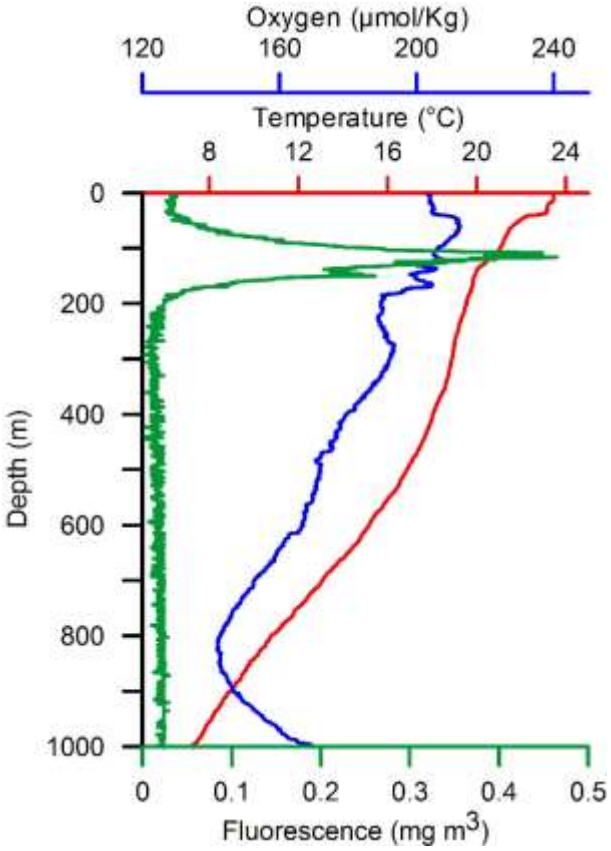

Figure 2: Plots of hydrographic conditions on 20 May 2021 at 32º 10.435N, 64° 30.018W (i.e., prior to Tow 1, Table 1). Additional hydrographic data are available at https://www.bco-dmo.org/project/764114.

569

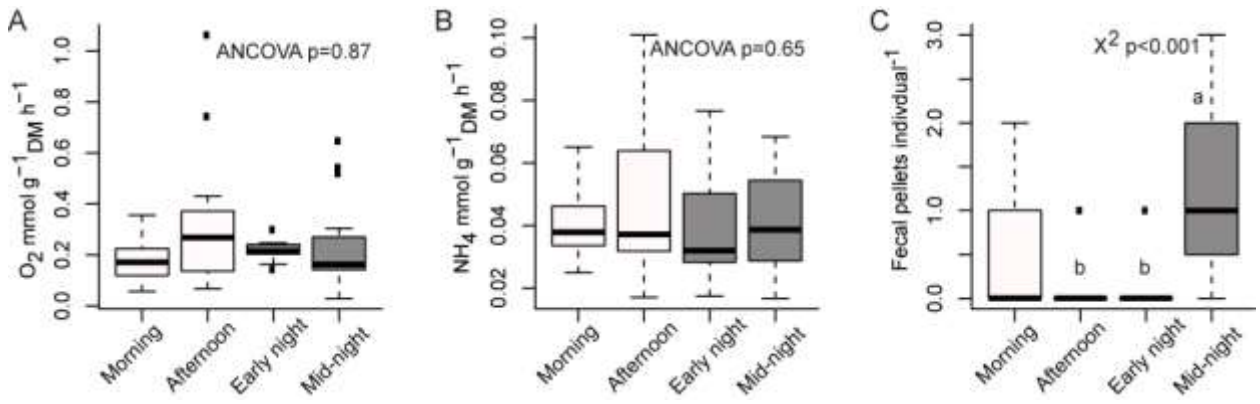

570

571 Figure 3: *Pleuromamma xiphias* physiological rates. Distinct letters indicate statistically distinct

572 time points. Open boxes denote samples collected from depth (400-600 m) during daytime, and

573 solid boxes indicate samples collected from surface waters (<200 m) during night. Oxygen and

574 ammonium rates per gram dry mass (DM) per hour. (A) Oxygen consumption, N=10-19; (B)

575 Ammonium excretion, N=10-18; (C) Fecal pellet production (per 3-hour incubation period),

576 N=13-19.

577

Figure 4: Examples of fecal pellets produced by *Pleuromamma xiphias* during 3-hour incubations over a three-day period, with sequential sampling points beginning in the upper left and proceeding to the right and down over time.

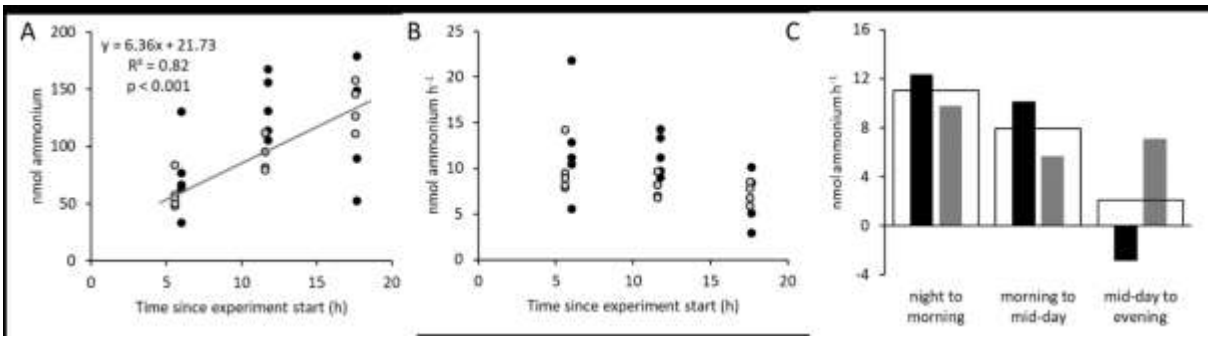

Figure 5: Time series of *Pleuromamma xiphias* ammonium production from individual copepods that had been captured between 19:45 and 22:45 on May 20th (solid symbols) or between 19:45 and 20:45 on May 22nd (open symbols). Both excretion experiments were set up at ~23:15 and results are reported as time since the start of the experiment (x-axis) with (A) total production; (B) production integrated over time on the y-axis; (C) production per 6-hour sampling window calculated by excluding the average production of the prior time points to demonstrate the excretion rate over the duration of the experiment in relation to solar time. White bars show the average production per time point.

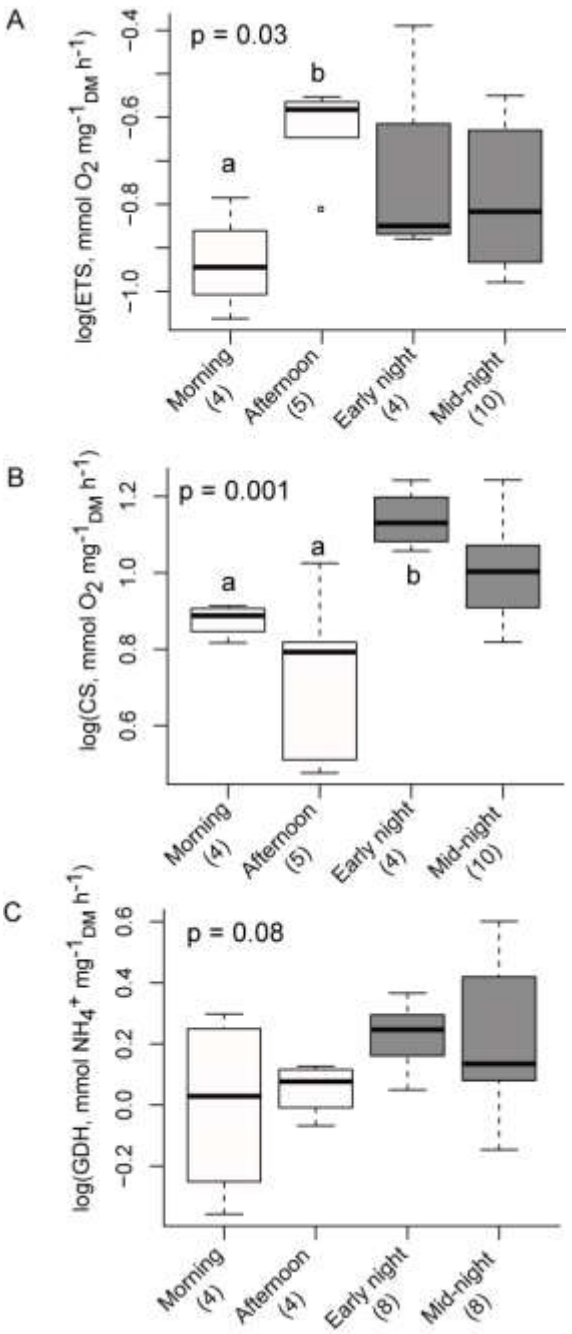

596

597 Figure 6: Log-transformed enzymatic activity per gram dry mass (DM). Time of sampling and
598 sample size indicated on the x-axis. Open boxes indicate samples collected from depth (400-600
599 m) during daytime, and shaded boxes indicate samples collected from surface waters (<200 m)
600 during night. Letters indicate statistically distinct time points. (A) Electron transport system, ETS
601 (B) Citrate synthase, CS; (C) glutamate dehydrogenase, GDH.

602

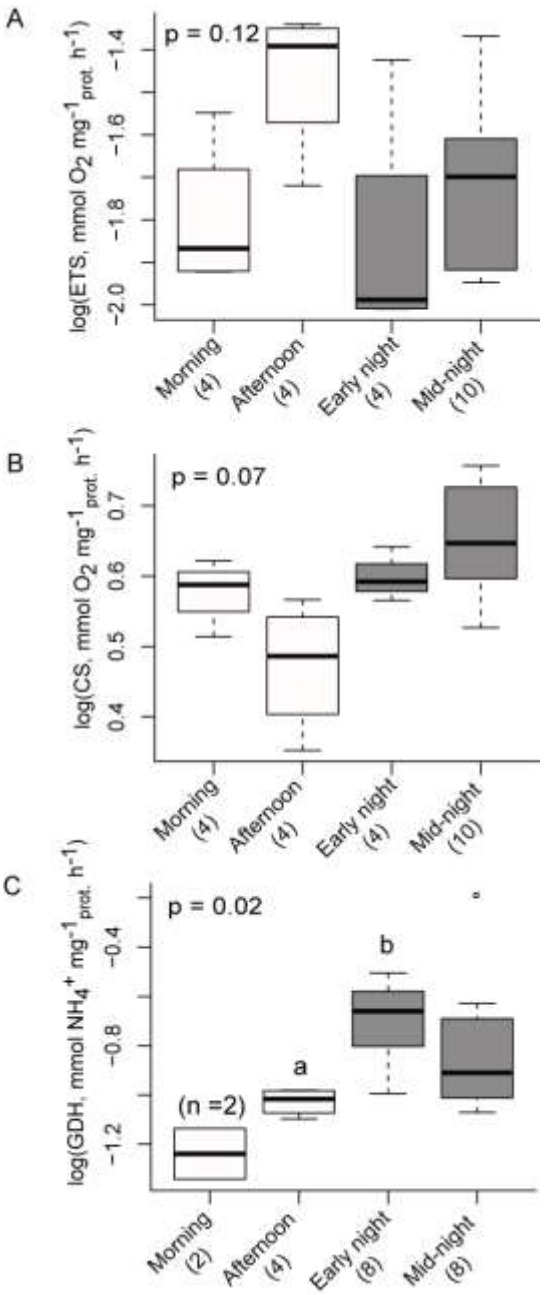

Supplemental Figure 1: Log-transformed enzymatic activity per mg of protein. Time of sampling and sample size indicated on the x-axis. Open boxes indicate daytime samples collected from depth (400-600 m), and shaded boxes indicate nighttime samples collected from surface waters (<200 m). Letters indicate statistically distinct time points. (A) Electron transport system, ETS (B) Citrate synthase, CS; (C) glutamate dehydrogenase, GDH.

609 References

610

611 Antezana, T. 2009. Species-specific patterns of diel migration into the Oxygen Minimum Zone
612 by euphausiids in the Humboldt Current Ecosystem. Progr. Oceanogr. 83: 228-236.
613 Aumont, O., O. Maury, S. Lefort, and L. Bopp. 2018. Evaluating the potential impacts of the
614 diurnal vertical migration by marine organisms on marine biogeochemistry. Global
615 Biogeochem. Cycles 32: 1622-1643.
616 Belcher, A., K. Cook, D. Bondyale-Juez, G. Stowasser, S. Fielding, R.A. Saunders, D.J. Mayor,
617 and G.A. Tarling. 2020. Respiration of mesopelagic fish: a comparison of respiratory
618 electron transport system (ETS) measurements and allometrically calculated rates in the
619 Southern Ocean and Benguela Current. ICES J. Mar. Sci. 77: 1672-1684.
620 Bianchi, D., C. Stock, E.D. Galbraith, and J.L. Sarmiento. 2013. Diel vertical migration:
621 Ecological controls and impacts on the biological pump in a one-dimensional ocean
622 model. Global Biogeochem. Cycles 27: 478-491.
623 Bidigare, R.R. 1983. Nitrogen excretion by marine zooplankton, in: Carpenter, E.J. , Capone
624 D.G. (Eds.), Nitrogen in the Marine Environment. Academic Press, New York. p. 385-
625 409. .
626 Biscontin, A., P. Martini, R. Costa, A. Kramer, B. Meyer, S. Kawaguchi, M. Teschke, and C. De
627 Pittà. 2019. Analysis of the circadian transcriptome of the Antarctic krill *Euphausia*
628 *superba*. Sci. Rep. 9: 1-11.
629 Blanco-Bercial, L., and A.E. Maas. 2018. A transcriptomic resource for the northern krill
630 *Meganyctiphanes norvegica* based on a short-term temperature exposure experiment.
631 Mar. Genom. 38: 25-32.
632 Bradford, M.M. 1976. A rapid and sensitive method for the quantitation of microgram quantities
633 of protein utilizing the principle of protein-dye binding. Anal. Biochem. 72: 248-254.
634 Burd, A., A. Buchan, M.J. Church, M.R. Landry, A.M. McDonnell, U. Passow, D.K. Steinberg,
635 and H.M. Benway. 2016. Towards a transformative understanding of the ocean's
636 biological pump: Priorities for future research. Report of the NSF Biology of the
637 Biological Pump Workshop, February 19-20, 2016 (Hyatt Place New Orleans, New
638 Orleans, LA), 67 pp., DOI:10.1575/1912/8263.
639 Burd, A.B., D.A. Hansell, D.K. Steinberg, T.R. Anderson, J. Arístegui, F. Baltar, S.R. Beaupre,
640 K.O. Buesseler, F. DeHairs, and G.A. Jackson. 2010. Assessing the apparent imbalance
641 between geochemical and biochemical indicators of meso-and bathypelagic biological
642 activity: What the@ $♯! is wrong with present calculations of carbon budgets? Deep-Sea
643 Res. Pt. II 57: 1557-1571.
644 Chow, S.-C., H. Wang, and J. Shao. 2007. Sample Size Calculations in Clinical Research. CRC
645 Press, New York.
646 Clarke, M., and P. Walsh. 1993. Effect of nutritional status on citrate synthase activity in *Acartia*
647 *tonsa* and *Temora longicornis*. Limnol. Oceanogr. 38: 414-418.
648 Crumbley, C., Y. Wang, S. Banerjee, and T.P. Burris. 2012. Regulation of expression of citrate
649 synthase by the retinoic acid receptor-related orphan receptor α (RORα). PLOS ONE 7:
650 e33804.
651 De Pittà, C., A. Biscontin, A. Albiero, G. Sales, C. Millino, G.M. Mazzotta, C. Bertolucci, and
652 R. Costa. 2013. The Antarctic krill *Euphausia superba* shows diurnal cycles of
653 transcription under natural conditions. PLOS ONE 8: e68652.

654 Díaz-Muñoz, M., O. Vázquez-Martínez, R. Aguilar-Roblero, and C. Escobar. 2000. Anticipatory
655 changes in liver metabolism and entrainment of insulin, glucagon, and corticosterone in
656 food-restricted rats. Am. J. Physiol.- Reg. I. 279: R2048-R2056.
657 Fernández-Urruzola, I., N. Osma, T.T. Packard, F. Maldonado, and M. Gómez. 2016. Spatio-
658 temporal variability in the GDH activity to ammonium excretion ratio in epipelagic
659 marine zooplankton. Deep-Sea Res. Pt. I 117: 61-69.
660 Fernández-Urruzola, I., T.T. Packard, and M. Gómez. 2011. GDH activity and ammonium
661 excretion in the marine mysid, *Leptomysis lingvura*: effects of age and starvation. J. Exp.
662 Mar. Biol. Ecol. 409: 21-29.
663 Freese, D., J.E. Søreide, and B. Niehoff. 2017. A year-round study on digestive enzymes in the
664 Arctic copepod *Calanus glacialis*: implications for its capability to adjust to changing
665 environmental conditions. Polar Biol. 39: 2241-2252.
666 Geiger, S.P., H.G. Kawall, and J.J. Torres. 2001. The effect of the receding ice edge on the
667 condition of copepods in the northwestern Weddell Sea: results from biochemical assays.
668 Hydrobiologia 453: 79-90.
669 Glatz, J., C. Baerwaldt, J. Veerkamp, and H. Kempen. 1984. Diurnal variation of cytosolic fatty
670 acid-binding protein content and of palmitate oxidation in rat liver and heart. J. Biol.
671 Chem. 259: 4295-4300.
672 Gliwicz, M.Z. 1986. Predation and the evolution of vertical migration in zooplankton. Nature
673 320: 746-748.
674 Goetze, E. 2011. Population differentiation in the open sea: insights from the pelagic copepod
675 *Pleuromamma xiphias*. Integr. Comp. Biol. 51: 580-597.
676 Häfker, N.S., B. Meyer, K.S. Last, D.W. Pond, L. Hüppe, and M. Teschke. 2017. Circadian
677 clock involvement in zooplankton diel vertical migration. Curr. Biol. 27: 2194-2201.
678 e2193.
679 Hawkins, T.D., J.C. Hagemeyer, K.D. Hoadley, A.G. Marsh, and M.E. Warner. 2016.
680 Partitioning of respiration in an animal-algal symbiosis: implications for different aerobic
681 capacity between *Symbiodinium* spp. Front. Physiol. 7: 128.
682 Hays, G.C. 2003. A review of the adaptative significance and ecosystem consequences of
683 zooplankton diel vertical migrations. Hydrobiologia 503: 163-170.
684 Hernández-León, S., S. Calles, and M.L.F. de Puelles. 2019a. The estimation of metabolism in
685 the mesopelagic zone: Disentangling deep-sea zooplankton respiration. Progr. Oceanogr.
686 178: 102163.
687 Hernández-León, S., and M. Gómez. 1996. Factors affecting the respiration/ETS ratio in marine
688 zooplankton. J. Plankton Res. 18: 239-255.
689 Hernández-León, S., M.P. Olivar, M.L. Fernández de Puelles, A. Bode, A. Castellón, C. López-
690 Pérez, V.M. Tuset, and J.I. González-Gordillo. 2019b. Zooplankton and micronekton
691 active flux across the tropical and subtropical Atlantic Ocean. Front. Mar. Sci. 6: 535.
692 Hernández-León, S., S. Putzeys, C. Almeida, P. Bécognée, A. Marrero-Díaz, J. Arístegui, and L.
693 Yebra. 2019c. Carbon export through zooplankton active flux in the Canary Current. J.
694 Mar. Syst. 189: 12-21.
695 Herrera, I., L. Yebra, T. Antezana, A. Giraldo, J. Färber-Lorda, and S. Hernández-León. 2019.
696 Vertical variability of *Euphausia distinguenda* metabolic rates during diel migration into
697 the oxygen minimum zone of the Eastern Tropical Pacific off Mexico. J. Plankton Res.
698 41: 165-176.

699 Holmes, R.M., A. Aminot, R. Kérouel, B.A. Hooker, and B.J. Peterson. 1999. A simple and
700 precise method for measuring ammonium in marine and freshwater ecosystems. Can. J.
701 Fish. Aquat. Sci. 56: 1801-1808.
702 Ikeda, T., J. Torres, S. Hernández-León, and S. Geiger. 2000. Metabolism. in: Harris, R.P.,
703 Wiebe, P.H., Lenz, J., Skjoldal, H.R., Huntley M. (Eds.), ICES Zooplankton
704 Methodology Manual. Academic Press, New York, pp. 455-532. .
705 Kiko, R., P. Brandt, S. Christiansen, J. Faustmann, I. Kriest, E. Rodrigues, F. Schütte, and H.
706 Hauss. 2020. Zooplankton-mediated fluxes in the eastern tropical North Atlantic. Front.
707 Mar. Sci. 7: 358.
708 Kiørboe, T., F. Møhlenberg, and K. Hamburger. 1985. Bioenergetics of the planktonic copepod
709 *Acartia tonsa*: relation between feeding, egg production and respiration, and composition
710 of specific dynamic action. Mar. Ecol. Prog. Ser. 26: 85-97.
711 Kobari, T., M. Kitamura, M. Minowa, H. Isami, H. Akamatsu, H. Kawakami, K. Matsumoto, M.
712 Wakita, and M. Honda. 2013. Impacts of the wintertime mesozooplankton community to
713 downward carbon flux in the subarctic and subtropical Pacific Oceans. Deep-Sea Res. Pt.
714 I 81: 78-88.
715 Kodama, T., K. Takahashi, K.-i. Nakamura, S. Shimode, T. Yamaguchi, and T. Ichikawa. 2015.
716 Short-term variation in the *Calanus sinicus* ammonium excretion rate during the post-
717 capture period. Plankton Benthos Res. 10: 75-79.
718 Le Borgne, R., and M. Rodier. 1997. Net zooplankton and the biological pump: a comparison
719 between the oligotrophic and mesotrophic equatorial Pacific. Deep-Sea Res. Pt. II 44:
720 2003-2023.
721 Longhurst, A., A. Bedo, W. Harrison, E. Head, and D. Sameoto. 1990. Vertical flux of
722 respiratory carbon by oceanic diel migrant biota. Deep-Sea Res. Pt. A 37: 685-694.
723 Longhurst, A.R., and W.G. Harrison. 1988. Vertical nitrogen flux from the oceanic photic zone
724 by diel migrant zooplankton and nekton. Deep-Sea Res. Pt. I 35: 881-889.
725 Maas, A.E., L. Blanco-Bercial, A. Lo, A.M. Tarrant, and E. Timmins-Schiffman. 2018.
726 Variations in copepod proteome and respiration rate in association with diel vertical
727 migration and circadian cycle. Biol. Bull. 235: 30-42.
728 Maas, A.E., S. Liu, L.M. Bolaños, B. Widner, R. Parsons, E.B. Kujawinski, L. Blanco-Bercial,
729 and C.A. Carlson. 2020. Migratory zooplankton excreta and its influence on prokaryotic
730 communities. Front. Mar. Sci. 7: 573268.
731 Maldonado, F., T. Packard, and M. Gómez. 2012. Understanding tetrazolium reduction and the
732 importance of substrates in measuring respiratory electron transport activity. J. Exp. Mar.
733 Biol. Ecol. 434: 110-118.
734 Meyer, B., L. Auerswald, V. Siegel, S. Spahić, C. Pape, B.A. Fach, M. Teschke, A.L. Lopata,
735 and V. Fuentes. 2010. Seasonal variation in body composition, metabolic activity,
736 feeding, and growth of adult krill *Euphausia superba* in the Lazarev Sea. Mar. Ecol.
737 Prog. Ser. 398: 1-18.
738 Osma, N., I. Fernández-Urruzola, M. Gómez, S. Montesdeoca-Esponda, and T. Packard. 2016.
739 Predicting in vivo oxygen consumption rate from ETS activity and bisubstrate enzyme
740 kinetics in cultured marine zooplankton. Mar. Biol. 163: 146.
741 Owens, T., and F. King. 1975. The measurement of respiratory electron-transport-system activity
742 in marine zooplankton. Mar. Biol. 30: 27-36.
743 Packard, T. 1985. Measurement of electron transport activity of microplankton. Adv. Aquat.
744 Microbiol. 3: 207-261.

745 Packard, T.T., and M. Gómez. 2013. Modeling vertical carbon flux from zooplankton
746 respiration. Progr. Oceanogr. 110: 59-68.
747 Packard, T.T., H.J. Minas, B. Coste, R. Martinez, M.C. Bonin, J. Gostan, P. Garfield, J.
748 Christensen, Q. Dortch, and M. Minas. 1988. Formation of the Alboran oxygen minimum
749 zone. Deep-Sea Res. Pt. I 35: 1111-1118.
750 Pavlova, E. 1994. Diel changes in copepod respiration rates. Hydrobiologia 292: 333-339.
751 Pinti, J., T. Kiørboe, U.H. Thygesen, and A.W. Visser. 2019. Trophic interactions drive the
752 emergence of diel vertical migration patterns: a game-theoretic model of copepod
753 communities. Proc. R. Soc. Lond. B 286: 20191645.
754 Reeve, M. 1981. Large cod-end reservoirs as an aid to the live collection of delicate zooplankton.
755 Limnol. Oceanogr. 26: 577-580.
756 Robinson, C., D.K. Steinberg, T.R. Anderson, J. Arístegui, C.A. Carlson, J.R. Frost, J.F.
757 Ghiglione, S. Hernández-León, G.A. Jackson, and R. Koppelmann. 2010. Mesopelagic
758 zone ecology and biogeochemistry -- a synthesis. Deep-Sea Res. Pt. II 57: 1504-1518.
759 Schnetzer, A., and D. Steinberg. 2002a. Natural diets of vertically migrating zooplankton in the
760 Sargasso Sea. Mar. Biol. 141: 89-99.
761 Schnetzer, A., and D.K. Steinberg. 2002b. Active transport of particulate organic carbon and
762 nitrogen by vertically migrating zooplankton in the Sargasso Sea. Mar. Ecol. Prog. Ser.
763 234: 71-84.
764 Siegel, D.A., K.O. Buesseler, M.J. Behrenfeld, C.R. Benitez-Nelson, E. Boss, M.A. Brzezinski,
765 A. Burd, C.A. Carlson, E.A. D'Asaro, and S.C. Doney. 2016. Prediction of the export and
766 fate of global ocean net primary production: The EXPORTS science plan. Front. Mar.
767 Sci. 3: 22.
768 Silver, R., P.D. Balsam, M.P. Butler, and J. LeSauter. 2011. Food anticipation depends on
769 oscillators and memories in both body and brain. Physiol. Behav. 104: 562-571.
770 Steinberg, D.K., C.A. Carlson, N.R. Bates, S.A. Goldthwait, L.P. Madin, and A.F. Michaels.
771 2000. Zooplankton vertical migration and the active transport of dissolved organic and
772 inorganic carbon in the Sargasso Sea. Deep-Sea Res. Pt. I 47: 137-158.
773 Steinberg, D.K., S.A. Goldthwait, and D.A. Hansell. 2002. Zooplankton vertical migration and
774 the active transport of dissolved organic and inorganic nitrogen in the Sargasso Sea.
775 Deep-Sea Res. Pt. I 49: 1445-1461.
776 Steinberg, D.K., and M.R. Landry. 2017. Zooplankton and the ocean carbon cycle. Ann. Rev.
777 Mar. Sci. 9: 413-444.
778 Steinberg, D.K., B.A. Van Mooy, K.O. Buesseler, P.W. Boyd, T. Kobari, and D.M. Karl. 2008.
779 Bacterial vs. zooplankton control of sinking particle flux in the ocean's twilight zone.
780 Limnol. Oceanogr. 53: 1327-1338.
781 Teschke, M., S. Wendt, S. Kawaguchi, A. Kramer, and B. Meyer. 2011. A circadian clock in
782 antarctic krill: an endogenous timing system governs metabolic output rhythms in the
783 euphausid species *Euphausia superba*. PLOS ONE 6: e26090.
784 Teuber, L., R. Kiko, F. Séguin, and H. Auel. 2013. Respiration rates of tropical Atlantic
785 copepods in relation to the oxygen minimum zone. J. Exp. Mar. Biol. Ecol. 448: 28-36.
786 Thuesen, E.V., C.B. Miller, and J.J. Childress. 1998. Ecophysiological interpretation of oxygen
787 consumption rates and enzymatic activities of deep-sea copepods. Mar. Ecol. Prog. Ser.
788 168: 95-107.

789 Willett, C.S., and R.S. Burton. 2003. Characterization of the glutamate dehydrogenase gene and
790 its regulation in a euryhaline copepod. Comp. Biochem. Physiol. B Biochem. Mol. Biol.
791 135: 639-646.
792 Zhang, X., and H.G. Dam. 1997. Downward export of carbon by diel migrant mesozooplankton
793 in the central equatorial Pacific. Deep-Sea Res. Pt. II 44: 2191-2202.

794